

Critical Interaction Strength for Surfactant-Induced Mesomorphic Structures in Polymer–Surfactant Systems

Janne Ruokolainen,[†] Mika Torkkeli,[‡] Ritva Serimaa,[‡] Sakari Vahvaselkä,[‡] Mika Saariaho,[†] Gerrit ten Brinke,^{*,†,§} and Olli Ikkala^{*,†}

Department of Technical Physics, Helsinki University of Technology, FIN-02150 Espoo, Finland, Department of Physics, University of Helsinki, P.O. Box 9, FIN-00014, Finland, and Laboratory of Polymer Chemistry and Materials Science Center, University of Groningen, Nijenborgh 4, 9747 AG Groningen, The Netherlands

Received December 5, 1995; Revised Manuscript Received June 17, 1996[®]

ABSTRACT: The critical interaction strength to induce mesomorphic structures in flexible polymers by complexing with surfactants is determined by using surfactants with different hydrogen-bonding strengths. Two essential requirements have to be satisfied: (i) the association has to be strong enough, otherwise the structure dissociates. (ii) The polar–nonpolar repulsion has to be sufficiently strong to induce microphase separation. If the latter requirement is not satisfied, but the association is sufficiently strong, a characteristic comb polymer-like SAXS peak will still be present in the homogeneous melt state. To address these issues experimentally, poly(4-vinylpyridine) (P4VP) was combined with different classes of hydrogen-bonding surfactants: alkyl aromatic alcohols, alkyl carboxylic acids, alkyl aliphatic alcohols, and alkyl aliphatic amines. FTIR, SAXS, WAXS, and optical microscopy demonstrate that alkyl aromatic alcohols, such as 1-dodecyl 3,4,5-trihydroxybenzoate yield mesomorphic structures at not too high a temperature. Alkyl carboxylic acids are somewhat less effective. In the melt state, the SAXS data still show a peak, but because no birefringence could be found, the peak is attributed to block copolymer-like concentration fluctuations in an otherwise homogeneous state. Aliphatic alkyl alcohols yield still weaker hydrogen bonding. In the melt the short alkyl aliphatic alcohol surfactants form a homogeneous mixture with P4VP, but a SAXS peak is no longer observed. The longer ones macrophase separate. Both the alkyl carboxylic acids and the short alkyl aliphatic alcohols partly macrophase separate at lower temperatures due to crystallization.

1. Introduction

Polymer properties can be modified by incorporating covalently bound side groups. The classic book by Platé and Shibaev¹ describes how flexible polymers are stiffened by a high concentration of alkyl side groups covalently bonded to the polymer backbone to form *comb shape polymers*. The stiffening is induced by the excluded volume effects of the flexible side groups. More rigid mesogenic side groups can also be covalently bonded to the flexible backbone to induce rigidity.² On the other hand, covalently bonded side groups can also be used to plasticize the polymer, i.e., to reduce its glass transition temperature. This phenomenon is particularly important when the polymer backbone is rigid. For example, polythiophenes and polyanilines are semirigid polymers, therefore being infusible and nonsoluble to common solvents due to their limited conformational entropy. Using covalently bonded alkyl side groups typically of length 6–16 CH₂ units, they can be plasticized to increase solubility and fusibility.^{3–5} In these cases also mesomorphic structures are reported. Similar behavior has been observed in a wide class of other alkyl-substituted rigid rod polymers.^{6–8}

Recently it has been reported that interesting properties can also be obtained by using strongly associating surfactants. Semirigid polymers such as polypyrrole and polyaniline can be rendered mesomorphic when suitable surfactants with long alkyl chains are complexed.^{9–11} In this case intractable polyaniline can be rendered soluble or fusible with an alkyl containing

surfactant^{10,12} with a reduced glass transition temperature.¹³ Also more special surfactants can be used, not containing alkyl chains: polyaniline (PANI) complexed with camphor sulfonic acid (CSA) yields exceptionally high solubility and liquid-crystalline structures in *m*-cresol.¹⁴ Recently it has been suggested that the synergistic phenomena of phenols with PANI (CSA) are due to the molecular recognition phenomena where *m*-cresol forms simultaneously both a hydrogen bond and a phenyl/phenyl interaction with the PANI (CSA) complex due to the steric fit.¹⁵ Motivated by biochemical systems, the more complete molecular recognition scheme is demonstrated for PANI in the case of resorcinol in combination with sulfonic acid doped PANI.¹⁶

In the case of more flexible polymers, polyelectrolyte/surfactant complexes have been studied only very recently. Poly(styrenesulfonate sodium salt) complexes with different types of cationic surfactants yield mesomorphic behavior in bulk.^{17–19} Poly(vinylpyridine) protonated by anionic surfactant dodecylbenzenesulfonic acid (DBSA) is mesomorphic in bulk and in xylene solution²⁰ which is a good solvent for the alkyl side chains. The xylene solvent induces considerable stretching of the alkyl chains, as suggested theoretically by Fredrickson.²¹ Coordination complexation can also yield mesomorphic structures as demonstrated by zinc dodecylbenzenesulfonate, i.e., Zn(DBS)₂, in combination with P4VP.²²

Here we want to address some key parameters governing the formation of self-assembled polymer/surfactant structures. Specifically, we will concentrate on the influence of the strength of the polymer–surfactant interaction and the length of the alkyl tail of the surfactant. For covalently bound side chains, the bonding is permanent (of the order 100 kcal/mol). In this case, whether or not mesomorphic structures are

[†] Helsinki University of Technology.

[‡] University of Helsinki.

[§] University of Groningen.

[®] Abstract published in *Advance ACS Abstracts*, August 15, 1996.

obtained depends on the various parameters involved in a manner that is well described by conventional block copolymer theory. The situation changes when the side chains are bonded only by secondary bondings: if the bond is too weak, it may energetically be more favorable to render macroscopic phase separation between the surfactant and the polymer. But even if macroscopic phase separation does not occur, a homogeneously mixed situation may be favored over self-organized structures that require considerable side-chain stretching. In the case of ionically bound surfactants, the expected strength of the interaction is high as is the polar–nonpolar repulsion, and mesomorphic behavior occurs almost invariably. In these cases, the presence of charges can strongly influence the morphology due to ionic clustering.²³

If one eliminates all charges and reduces the interaction strength, a situation arises with two essential differences: first, the system is no longer of a polyelectrolyte nature, and second, the dynamic aspects of the polymer/surfactant enter the picture. The surfactant/polymer complexation cannot be regarded as permanent, but bonds are continuously broken and re-formed. Therefore, if mesomorphic structures occur at all in this case, and we know that they do in some cases,^{24–26} the morphology may be different from the strong bonding limit. A typical hydrogen bond has the strength of the order of a few kcal/mol which is 1 or 2 orders of magnitude less than that of an ionic or covalent bond. When the interaction is still further reduced, the surfactant and the polymer will ultimately macrophase separate. For intermediate strength interactions, a homogeneous state prevails. This homogeneous state may still show a distinct SAXS peak due to characteristic block copolymer-like concentration fluctuations, but this will obviously depend on the average hydrogen-bond lifetime.²⁷

This paper discusses experiments involving different classes of surfactants capable of hydrogen bonding with poly(vinylpyridine). Depending on the nitrogen atom position, two isomeric forms of poly(vinylpyridine) are used: poly(2-vinylpyridine) (P2VP) with $T_g = 104\text{ }^\circ\text{C}$ and poly(4-vinylpyridine) (P4VP) with $T_g = 148\text{ }^\circ\text{C}$. Both are soluble and fusible and, therefore, differ essentially from semirigid polymers, such as polyaniline or poly(2,6-dimethyl-1,4-phenylene). Most results will refer to P4VP because of the favorable position of the basic nitrogen. The functional groups of the surfactants investigated are aromatic alcohols, i.e., phenols, carboxylic acids, aliphatic alcohols, and aliphatic amines. The phenolic surfactants are somewhat acidic with $pK_a = 10$ due to the aromatic ring whereas aliphatic alcohols are nonacidic with $pK_a = 15\text{--}17$. Carboxylic acids are further examples of acidic surfactants which, however, show strong intermolecular association. The results are compared to the behavior seen for the strong acid DBSA which has an ionic interaction with P2VP and P4VP,²⁰ its zinc salt, i.e., $\text{Zn}(\text{DBS})_2$ forming a coordination complex with P4VP,²² and the 3-pentadecylphenol (PDP) complexes with P4VP based on hydrogen bonding and reported in our recent publication.²⁴ Theoretical arguments explaining the intricate phase behavior of P4VP-PDP, notably the decrease of the long period of the lamellar structure as a function of the amount of PDP, have been discussed.^{24,28}

We will start our discussion with a brief analysis of the essential parameters involved in the formation of mesomorphic structures. Then the numerical estimates

of the interaction strengths between P4VP and the different surfactants will be presented. Together, these will form the basis on which to discuss and explain our experimental results.

2. Experimental Section

Materials. The atactic P2VP and atactic P4VP were acquired from Polyscience Europe GmbH. The molar masses of P2VP ($M_v = 330\,000\text{ g mol}^{-1}$) and P4VP ($M_v = 49\,000\text{ g mol}^{-1}$) were determined by viscometry in DMF using²⁹ $[\eta] = 1.47 \times 10^{-4} M_v^{0.67}$ and in absolute ethanol using³⁰ $[\eta] = 2.5 \times 10^{-4} M_v^{0.68}$, respectively. 3-Pentadecylphenol (PDP) was purchased from Aldrich, and 1-dodecyl 3,4,5-trihydroxybenzoate, i.e., lauryl gallate (LG), from Nipa Industries. All other surfactants were obtained from Fluka. All surfactants are of highest available purity. Ethanol, DMF, and chloroform were of analysis grade. All solvents used were carefully dried by 3 Å molecular sieves.

Sample Preparation. P4VP and P2VP were first dried at $60\text{ }^\circ\text{C}$ in vacuum for 2 days. Also the surfactant materials were dried at $60\text{ }^\circ\text{C}$ in vacuum at least 1 day. P4VP-(surfactant), and P2VP-(surfactant), complexes were prepared from DMF solutions, unless otherwise stated. Here x denotes the number of surfactant molecules per vinylpyridine repeat unit. We will consider mostly the nominally fully complexed case, i.e., $x = 1.0$. In each case, the surfactant and the solvent were first mixed together until a clear solution was obtained. P4VP or P2VP was subsequently added, followed by mechanical stirring for approximately 1 h at a $60\text{ }^\circ\text{C}$. The concentrations were kept low (less than 2.5 w/w %) to ensure homogeneous complex formation. DMF or other solvents were first evaporated on a hot plate at $70\text{ }^\circ\text{C}$. Whenever chloroform was used, the stirring was performed at room temperature due to the rapid evaporation. The complexes were further dried at $60\text{ }^\circ\text{C}$ in vacuum at least for 2 days and thereafter stored in a desiccator.

Small-Angle X-Ray Scattering. A sealed fine-focus Cu X-ray tube was used in a point focusing mode. The Cu K α ($\lambda = 1.542\text{ \AA}$) radiation is monochromatized with a Ni filter and a totally reflecting glass block (Huber small-angle chamber 701). The scattered radiation is detected in the horizontal (beam width) direction by a linear one-dimensional proportional counter (MBraun OED-50M). The space between sample and detector is evacuated to 0.05 mmHg using $13\text{ }\mu\text{m}$ polyimide foils as X-ray windows. The beam height is limited by two horizontal slits with approximately 1 mm aperture, one before the sample and another in front of the detector. Also, a narrow vertical slit is placed before the sample to reduce background scattering. The fwhm of the beam width is below 0.002 \AA^{-1} and the instrumental function in the vertical direction, due to beam height and detector height profiles, is determined to have fwhm = 0.048 \AA^{-1} . Owing to this, no correction for the experimental smearing is necessary in the current analysis. The small-angle scattering was recorded at various temperatures.

Wide-Angle X-ray Scattering. Transmission diffraction measurements were performed on pressed pellets having a thickness of 1 mm and diameter of 20 mm, at $20\text{ }^\circ\text{C}$ under atmospheric conditions. The measurements were predominantly made with a Seifert ID 3000 diffractometer using monochromatic Mo K α ($\lambda = 0.7096\text{ \AA}$) and a scintillation counter. The P4VP(carboxylic acid)_{1,0} complexes were measured by another vertical diffractometer³¹ using Mo K α radiation monochromatized with a Si(220) monochromator in the incident beam and a solid-state (SSD HP Ge) detector. The air scattering was reduced by enclosing the sample in a vacuum chamber. The magnitude of the scattering vector k was calculated from the scattering angle 2θ using the relation $k = 4\pi \sin \theta/\lambda$.

Infrared Spectroscopy. Infrared spectra were obtained using a Nicolet 750 FTIR spectrometer. Samples were prepared from chloroform or DMF solution on potassium bromide crystals. All measurements are taken at room temperature.

Computational Methods. The bonding energy between an individual chain of P4VP and one surfactant molecule was

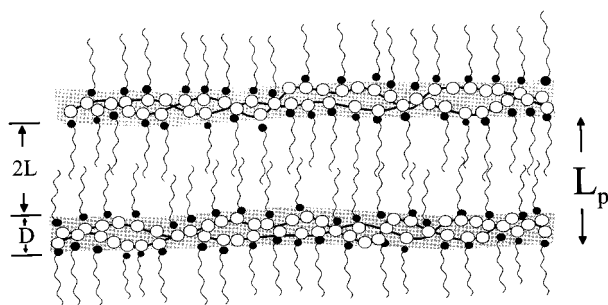


Figure 1. Lamellar model for polymer/surfactant system.

calculated using Insight software by Biosym Technologies.³² To simplify calculations, the polymer chains were limited to consist of only three monomer units with methyl group termination at both ends to suppress the chain end effects. All surfactants were modeled containing the particular functional group in combination with an alkyl tail of four methyl units.

3. Results and Discussion

3.1. Theoretical Considerations. In dealing with polymer–surfactant systems, various types of “phase” behavior can be anticipated. Within the highly viscous fluid state, at least four different regimes can be defined: (I) microphase separated mesomorphic state; (II) homogeneous state showing a distinct SAXS peak; (III) homogeneous state without a clear SAXS peak; (IV) macrophase separated state.

The difference between II and III depends on the characteristic relaxation times, i.e., the average lifetime τ_b of a hydrogen bond and the relaxation time τ_f of the characteristic concentration fluctuations of the comblike block copolymer structure. If τ_b is of the order of τ_f or larger, the comblike structure is permanent on the time scale of the relevant concentration fluctuations and a characteristic block copolymer-like SAXS peak will be present.^{33–35} In the case of sufficiently strong association, regime I or II is found depending on the alkyl length and the polar–nonpolar alkyl–polymer complex repulsion.³⁶ We will demonstrate that all four possibilities actually occur for the surfactants under consideration.

Before presenting the experimental results, we first discuss briefly the essential parameters involved. In ref 28, the case of a microphase-separated lamellar structure, as illustrated in Figure 1, was analyzed in terms of the parameter x representing the number of surfactant molecules per polymer segment. The free energy of this type of structures contains three contributions, the stretching of the side chains, the interface interactions, and the polymer confinement. These last two terms are actually incorporated in a single interface free energy term. Minimization of the free energy for a given value of x demonstrated that the surfactant layer thickness $2L$ is almost invariant, whereas the polymer layer thickness D is proportional to $1/x$. The reason can be easily understood. A decrease in the polymer layer thickness increases the amount of interface, but the interfacial tension remains the same. Therefore, in response to an increase in the amount of surfactant, the system increases its interface in the same proportion. As a consequence, the long period is predicted to decrease as

$$L_p \propto x^{-1} \quad (1)$$

just as observed experimentally for the P4VP(PDP)_x

Table 1. Calculated Relative Interaction Strengths between Surfactants (A) Comprising Different Hydrogen-Bonding Donors and a Model Compound (B) Consisting of Three 4-Vinylpyridine Repeat Units

model surfactant (A)	E_{AB} (au)	E_{AA} (au)	$E_{AB} - 1/2 E_{AA}$ (au)
1-C ₄ H ₉ C ₆ H ₄ -3,4,5-(OH) ₃	-25.0	-24.5	-12.8
1-C ₄ H ₉ C ₆ H ₄ -4-OH	-18.8	-9.7	-14.0
C ₄ H ₉ COOH	-16.4	-13.1	-9.9
C ₄ H ₉ OH	-13.1	-8.2	-9.0
C ₄ H ₉ NH ₂	-8.0	-3.6	-6.2

system. From the results presented in ref 24, it is straightforward to derive the following expression for the free energy per unit volume of the lamellar structure:

$$f \cong x \frac{1}{1 + xn} \frac{\chi^{1/3} n^{1/3}}{a^3} kT \quad (2)$$

where n is the number of side chain segments, χ the Flory–Huggins interaction parameter describing the side chain–polymer interaction, and a^3 the volume of a segment. If it is assumed that the surfactant–polymer interaction ϵ has to offset at least this increase in free energy, we obtain

$$\epsilon \cong (\chi n)^{1/3} kT \quad (3)$$

The analysis is admittedly crude but does demonstrate that longer surfactant molecules require stronger surfactant–polymer interaction to sustain mesomorphic structures, the basic reason being the increase in stretching free energy. In reality, we do not believe that the structure is as perfect as sketched in Figure 1. We expect at least some of the polymer chains to transverse from one layer to another. Also, other structures than lamellar are possible. These observations do not invalidate, however, the general conclusion drawn from eq 3.

To compare the hydrogen-bonding ability of the surfactants involved, these interaction strengths were estimated numerically by using simple models, where a P4VP model compound (B) consisting of three repeat units is complexed with model surfactants (A) with alkyl tails of four methyl units. The energy gain due to complexation between A and B can be calculated by $\Delta E = E_{AB} - 1/2(E_{AA} + E_{BB})$. The structure consisting of one surfactant model molecule A and polymer model molecule B is first optimized to obtain their association energy E_{AB} . Similarly E_{AA} is calculated for two surfactant model molecules. The same method can be used to calculate E_{BB} for two polymer molecules. However, because in the calculation of ΔE , E_{BB} is a constant factor for all the cases involved, it is not really required. To gain more accurate results, the whole chains with their conformational entropy and even their packing should be considered, which is clearly a laborious task. With our simplified scheme, we do obtain a rough relative scale of the interactions by comparing the values of $E_{AB} - 1/2 E_{AA}$. The results are presented in Table 1. It suggests that the hydrogen-bonding capability decreases in the order phenol, carboxylic acid, aliphatic alcohol, amine. The table further shows that carboxylic acids have large intermolecular association, thus reducing the net interaction. However, as we have argued, the lifetime of a hydrogen bond is an essential parameter and the calculations indicate that this time will be considerably larger for the alkyl carboxyl acid surfac-

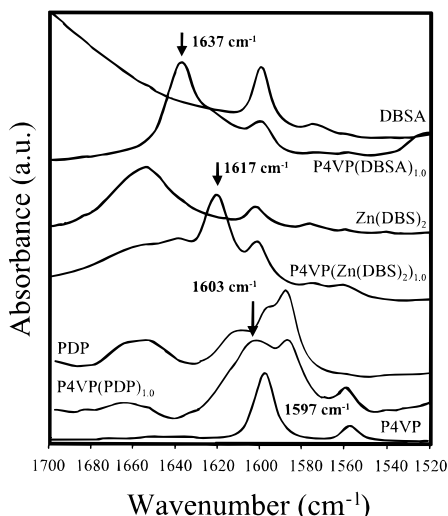


Figure 2. Infrared spectra illustrating the shifts of the 1597 cm^{-1} stretching band of P4VP upon nominally full complexation with *p*-dodecylbenzenesulfonic acid,²⁰ zinc dodecylbenzenesulfonate,²² and 3-pentadecylphenol.²⁴

tants than for the alkyl aliphatic alcohol surfactants. Trihydroxybenzoate has the largest interaction energy with P4VP but its intermolecular association is also strong. In fact, as will become clear, the trends predicted by these calculations are in full agreement with the experimental findings to which we will turn now.

3.2. Experimental Results. FTIR is used to investigate the hydrogen bonding of surfactants to poly(vinylpyridine). Previously, hydrogen bonding of OH group containing polymers to poly(vinylpyridines) have been investigated.^{37–39} Hydrogen-bonded alcohols⁴⁰ and poly(ethylene-*co*-methacrylic acid)⁴¹ show that hydrogen-bonding shifts the bands related to the stretching modes of the pyridine ring, i.e., 1590 and 993 cm^{-1} for P2VP and 1597 and 993 cm^{-1} for P4VP, to higher frequencies due to formation of stronger bonds. In the following the emphasis is on these bands.

Aromatic Alcohols: Alkylphenol Surfactants. *3-Pentadecylphenol.* Figure 2 summarizes as a reference for the discussions to follow our previously obtained FTIR data at the 1600 cm^{-1} band for P4VP nominally fully complexed with three different types of surfactants, each having different types of interactions and each yielding mesomorphic structures: 3-pentadecylphenol (PDP),²⁴ $\text{Zn}(\text{DBS})_2$,²² and DBSA.²⁰ A strong acid such as DBSA is capable of protonating, i.e., quaternizing the pyridine ring to form a pyridinium ring. In this case the acidic proton of DBSA is completely transferred to the pyridine ring. The interaction has strongly ionic character between the positively charged pyridinium ring and negatively charged sulfonate anion. Therefore, a polyelectrolyte is obtained. The strong bonding is manifested in FTIR: in pristine P4VP the pyridine ring has a stretching band at 1597 cm^{-1} . Upon nominally full complexation, this band is observed to shift to 1637 cm^{-1} corresponding to the formation of a pyridinium ring. In conclusion, a large shift of 40 cm^{-1} is observed. In the case of $\text{Zn}(\text{DBS})_2$, a coordination complexation is observed,²² the corresponding shift being only 20 cm^{-1} to 1617 cm^{-1} , suggesting a weaker bonding. In particular, a charged pyridinium ring is not formed. The same observation is valid also for PDP in which case a hydrogen bonding between the basic pyridine of P4VP and OH group of phenol yields only a small shift to 1603 cm^{-1} .²⁴ In the latter case, due to the over-

lapping peaks, the 1600 cm^{-1} band does not easily allow conclusions whether a full complexation is achieved. However, the 993 cm^{-1} band is observed to shift completely to 1008 cm^{-1} which shows that by application of 1 mol PDP vs 1 mol P4VP repeat units, a full complexation is achieved.

The hydrogen bonding between the phenol group and P4VP has been shown to be sufficiently strong to yield mesomorphic structures of $\text{P4VP}(\text{PDP})_x$ at room temperature. At elevated temperatures, a SAXS peak is still present, but the system is actually homogeneous.²⁷ The peak, well-known for ordinary block copolymers, is also here due to the block copolymer-like structure of the polymer-surfactant complexes. Furthermore, SAXS measurements show that, being noncharged, i.e., non-polyelectrolyte, conceptually different structures in $\text{P4VP}(\text{PDP})_x$ are obtained at low degrees of complexation compared to the charged systems $\text{P4VP}(\text{Zn}(\text{DBS})_2)_x$ and $\text{P4VP}(\text{DBSA})_x$.²⁴

Lauryl Gallate. To investigate the effect of several hydroxyl groups in the phenol moiety of the surfactant and to potentially achieve even more hydrogen bonding, lauryl gallate (LG) was selected. It is a crystalline material with a melting point of 97 °C.

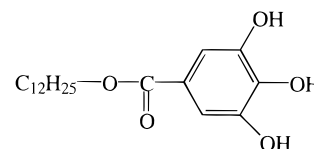


Figure 3a shows that the 993 cm^{-1} stretching band of the pyridine ring is completely shifted to 1010 cm^{-1} for $\text{P4VP}(\text{LG})_{1.0}$, indicating essentially complete complexation. Figure 3b shows that also the 1597 cm^{-1} band is shifted to higher wavenumbers upon hydrogen bonding. Reducing x from 1.0 to 0.5 has only very little influence on the spectra, demonstrating that LG is indeed capable of hydrogen bonding with more than one pyridine group at the same time. For smaller values of x , the complexation gradually decreases. The FTIR results for $\text{P4VP}(\text{LG})_{1.0}$ resemble those of $\text{P4VP}(\text{PDP})_{1.0}$, indicating a comparable strength of the interactions. Figures 4 and 5 show SAXS and WAXS results of $\text{P4VP}(\text{LG})_x$ for $x = 1.0, 0.5, 0.25$, of $\text{P2VP}(\text{LG})_x$ for $x = 1.0$ and 0.5 and of pure LG. All samples are prepared in the same manner. As confirmed by optical microscopy (birefringence), all $\text{P4VP}(\text{LG})_x$ samples are mesomorphic at room temperature with a long period increasing from 32.4 to 35.5 to 37.4 Å for $x = 0.25, 0.5$, and 1.0, respectively. The increase of the long period for increasing amounts of surfactant LG came as a big surprise. Previously, we observed exactly the opposite behavior in the case of PDP. This latter behavior with respect to the long period of the microphase-separated structure as well as for the wavelength of the dominant fluctuation in the homogeneous state above the order-disorder transition is exactly what is predicted for comb polymers as a function of the number of combs. Also there the periodicity decreases for increasing number of combs, essentially due to a decrease in lateral size of the polymer backbone.³⁶ For P4VP-PDP this was briefly discussed in section 3.1. We attribute the unexpected behavior of P4VP-LG tentatively to the multi functionality of LG, giving rise to physical cross links and therefore to different structures. For P2VP the situation is similar with a layer thickness of 34.1 and 31.7 Å

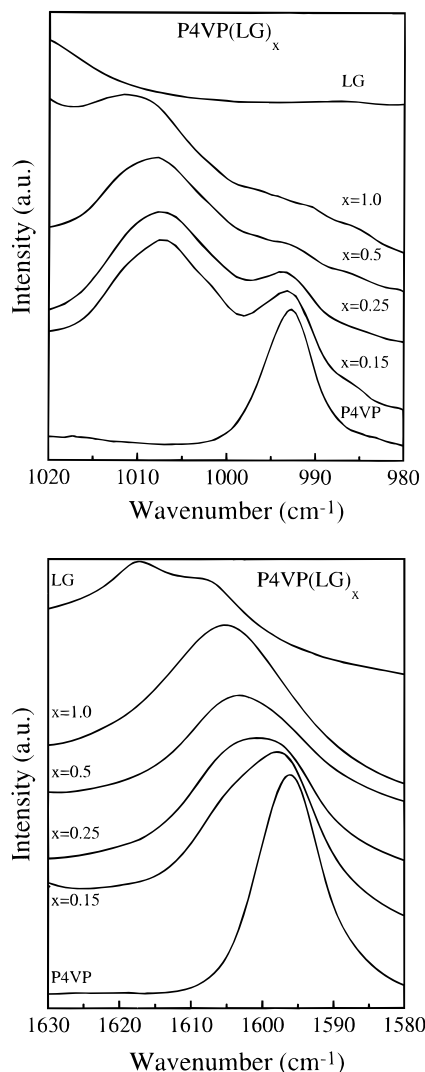


Figure 3. (a, top) Infrared spectra in the 1000 cm^{-1} region for P4VP(LG)_x , LG, and P4VP. (b, bottom) Infrared spectra in the 1600 cm^{-1} region for P4VP(LG)_x , LG, and P4VP. $x = 0.15, 0.25, 0.5, 1.0$. LG = 1-dodecyl 3,4,5-trihydroxybenzoate.

for $x = 1.0$ and 0.5 , respectively. The layer thicknesses are slightly smaller than for P4VP, as might be expected.

No clear crystalline WAXS peaks are visible, so the birefringence is not due to crystallization. Furthermore, the SAXS results at room temperature are very similar to those in the melt below 80°C not presented here. Also in the melt the samples are birefringent. Since, a SAXS peak in itself is insufficient evidence for a mesomorphic structure, the observed birefringence at room temperature and in the melt is essential for the conclusion that both P4VP-LG and P2VP-LG are microphase separated (preliminary results indicate an order-disorder transition around 80°C for $\text{P4VP(LG)}_{1.0}$).

Alkylcarboxylic Acid Surfactants. Alkyl carboxylic acids have been selected as further examples of moderately acidic surfactants. As compared with the alkyl phenols with the OH group attached to the phenyl groups, alkyl carboxylic acids are compounds where the phenyl group has been replaced by a carbonyl CO group. Complexes were made with P4VP using dodecanoic $\text{C}_{11}\text{H}_{23}\text{COOH}$ (DDA), hexadecanoic $\text{C}_{15}\text{H}_{31}\text{COOH}$ (HDA), and nonadecanoic $\text{C}_{18}\text{H}_{37}\text{COOH}$ (NDA) acids, each of which is crystalline. Their melting points are 44.2 , 63.1 , and 68.6°C , respectively.

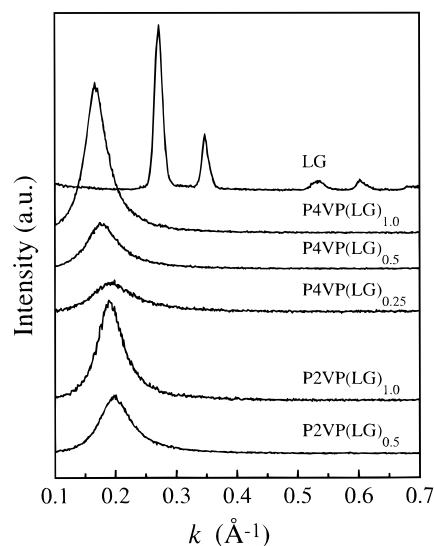


Figure 4. SAXS data for P4VP(LG)_x , $x = 0.25, 0.5$, and 1.0 , P2VP(LG)_x , $x = 0.5$ and 1.0 and pure LG. LG = 1-dodecyl 3,4,5-trihydroxybenzoate.

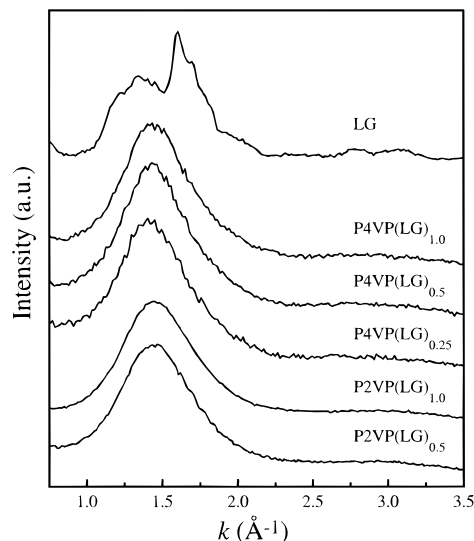


Figure 5. WAXS data for P4VP(LG)_x , $x = 0.25, 0.5$, and 1.0 , P2VP(LG)_x , $x = 0.5$ and 1.0 and pure LG. LG = 1-dodecyl 3,4,5-trihydroxybenzoate.

Figure 6a,b shows that upon addition of 1 mol of dodecanoic acid vs P4VP repeat units, the pyridine stretching bands at 993 and 1597 cm^{-1} are split into double peaks. Because part of IR absorption remains at the wavenumbers corresponding to pristine P4VP, it can be concluded that complete complexation is not achieved. This is in contrast with alkylphenol complexes with P4VP, where no absorption at the original wavenumber can be resolved. Figure 6b shows that for the hexadecanoic acid complex the intensities of shifted peaks become smaller and eventually for nonadecanoic acid complex the absorption is the same as pure P4VP. This is in agreement with visual inspection which suggests that hexadecanoic and nonadecanoic acids macroscopically phase separate from P4VP. However, the macro phase separation is due to crystallization since all systems appear homogeneous one phase in the melt at 100°C . Figure 7 shows the WAXS data of the pure carboxylic acids and their 1:1 mol complexes with P4VP at room temperature. All curves show a clear peak at the same position, indicating that crystallization has occurred. In the inset to this figure, the SAXS data for $\text{P4VP(HDA)}_{1.0}$ and pure HDA taken at room tem-

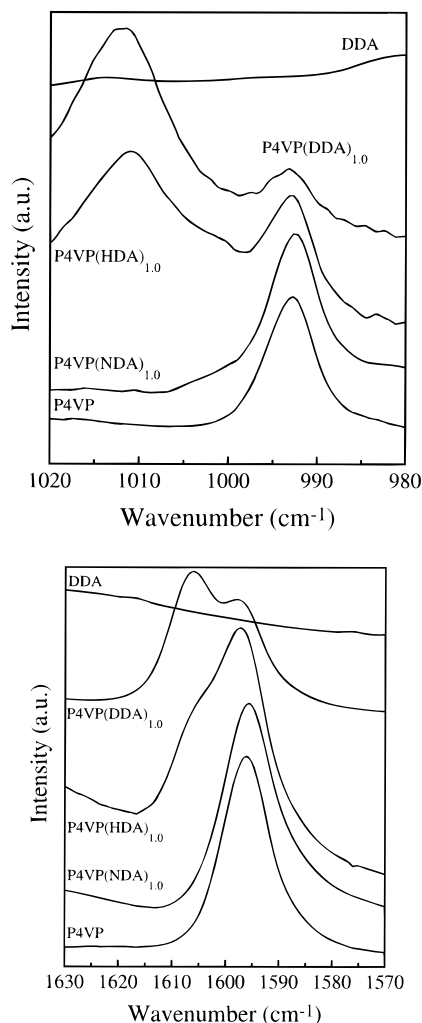


Figure 6. (a, top) Infrared spectra in the 1000 cm^{-1} region for $\text{P4VP(DDA)}_{1.0}$, $\text{P4VP(HDA)}_{1.0}$, $\text{P4VP(NDA)}_{1.0}$, P4VP , and DDA . (b, bottom) Infrared spectra of the same samples in the 1600 cm^{-1} . DDA = dodecanoic acid, HDA = hexadecanoic acid, NDA = nonadecanoic acid.

perature are presented. Although the results are very similar, as expected on the basis of the FTIR results, the peak of $\text{P4VP(HDA)}_{1.0}$ does become rather asymmetric due to the presence of P4VP .

Figure 8 shows the SAXS curves of the three different systems taken in the melt, i.e., above the crystallization temperatures of the surfactants involved. In all cases a clear maximum is observed. However, because birefringence could be induced in none of these systems, we conclude tentatively that the peaks correspond to the characteristic block copolymer-like concentration fluctuations in an otherwise homogeneous system. This conclusion is corroborated by our experience with P4VP-PDP and P4VP-LG . In both these systems birefringence is present in the melt at not too high temperatures. Moreover, as mentioned before, we have found very recently with time-resolved SAXS that $\text{P4VP(PDP)}_{1.0}$ undergoes an order-disorder transition around $60\text{ }^{\circ}\text{C}$,²⁷ which roughly corresponds to the temperatures required for the melt state, at least for HDA and NDA . The wavelength that corresponds to the peak positions is 30.6 , 35.5 , $39.5\text{ }\text{\AA}$ for dodecanoic acid, hexadecanoic acid, and nonadecanoic acid, respectively. The increase in wavelength as a function of the alkyl length is in good agreement with random phase approximation calculations for comb polymers.³⁶

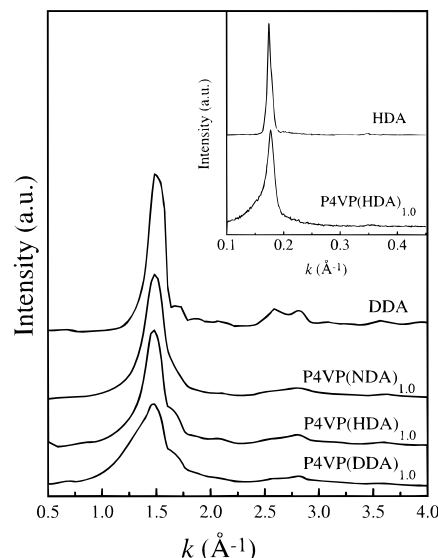


Figure 7. WAXS data for $\text{P4VP(DDA)}_{1.0}$, $\text{P4VP(HDA)}_{1.0}$, $\text{P4VP(NDA)}_{1.0}$, and pure DDA at room temperature. Inset SAXS of $\text{P4VP(HDA)}_{1.0}$ and pure HDA at room temperature. DDA = dodecanoic acid, HDA = hexadecanoic acid, NDA = nonadecanoic acid.

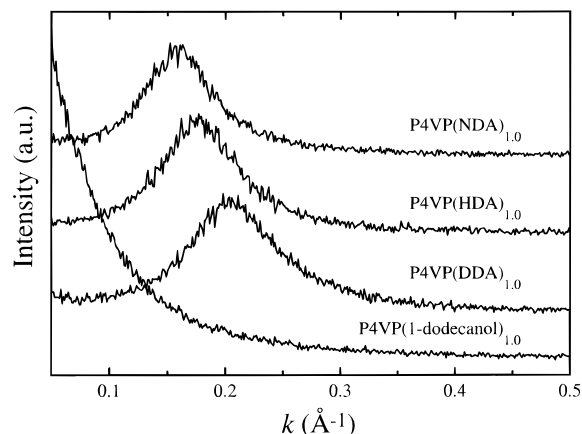


Figure 8. SAXS data for $\text{P4VP(DDA)}_{1.0}$, $\text{P4VP(HDA)}_{1.0}$, $\text{P4VP(NDA)}_{1.0}$, and $\text{P4VP(dodecanol)}_{1.0}$ taken in the melt at $100\text{ }^{\circ}\text{C}$. DDA = dodecanoic acid, HDA = hexadecanoic acid, NDA = nonadecanoic acid.

In conclusion, we see that alkyl carboxylic acids have sufficiently strong hydrogen-bonding ability to P4VP to induce comblike structures that are "permanent" on the time scale of the relaxation time of the characteristic concentration fluctuations. However, the repulsive polar-nonpolar interaction seems to be too small to actually form mesomorphic structures. These systems therefore classify as regime II surfactants.

Aliphatic Alcohols: Alkyl Alcohol Surfactants. Pure OH groups are essentially nonacidic with $\text{p}K_a=15-17$. Three aliphatic alcohols with different alkyl chain lengths were used: dodecanol ($\text{C}_{12}\text{H}_{25}\text{OH}$), hexadecanol ($\text{C}_{16}\text{H}_{33}\text{OH}$), and docosanol ($\text{C}_{22}\text{H}_{45}\text{OH}$). Their complexes with P4VP were prepared with molar ratios 1:1. Due to observed phase separation during DMF evaporation, all complexes were reproduced from both ethanol and chloroform. Figure 9a,b shows that for dodecanol complex the pyridine stretching bands of 993 and 1597 cm^{-1} are split into two peaks, a large portion of absorption being at the unshifted wavenumber. This observation shows that a large fraction of the pyridine rings are uncomplexed due to insufficient hydrogen-bonding strength. When the length of the alkyl chain

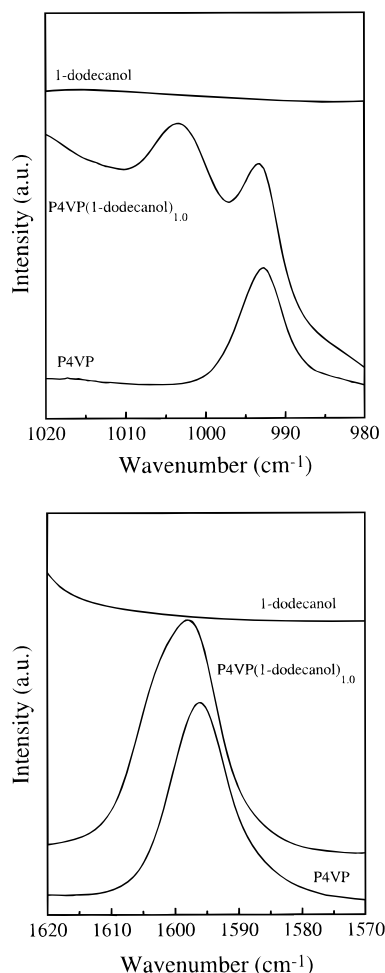


Figure 9. (a, top) Infrared spectra in the 1000 cm^{-1} region for P4VP(dodecanol)_{1.0}, 1-dodecanol, and P4VP. (b, bottom) Infrared spectra in the 1600 cm^{-1} region for the same samples.

is increased, macroscopic liquid–liquid phase separation takes place, as shown for hexadecanol and docosanol based on visual examination. P4VP was miscible with dodecanol, but, as shown in Figure 8, a SAXS peak was no longer observed. Hence, dodecanol falls in regime III, whereas the longer ones classify as IV.

The hydrogen bonding of the aliphatic alcohols to the pyridine nitrogens is marginal. It can easily be understood because hydrogen bonding is an acid/base interaction which is small in this case due to the small acidity of the aliphatic alcohol group. Therefore, very short-chain alcohols, such as methanol and ethanol up to dodecanol, yield solubility of P4VP and surfactants with longer alkyl chains give rise to liquid–liquid phase separation.

Aliphatic Amines: Alkylamine Surfactants. Dodecylamine ($\text{C}_{12}\text{H}_{25}\text{NH}_2$) and hexadecylamine ($\text{C}_{16}\text{H}_{33}\text{NH}_2$) were selected as representative surfactants from this group. Complexes between P4VP and aliphatic amines were prepared from both DMF and ethanol. In all cases the samples were macrophase separated in the melt. This indicated that the amine groups do not interact strongly enough with pyridine to yield miscibility.

4. Concluding Remarks

In this work the critical polymer/surfactant interaction strength to achieve mesomorphic structures based on flexible polymers and alkyl-containing surfactants

is studied experimentally. Poly(4-vinylpyridine) was selected as the polymeric model system. Surfactants with different hydrogen-bonding donor moieties were used. SAXS combined with optical microscopy confirmed that phenolic surfactants, such as 1-dodecyl 3,4,5-trihydroxybenzoate and the previously investigated pentadecylphenol, yield mesomorphic structures. Hence, they form sufficiently strong hydrogen bonds in combination with sufficiently strong polar–nonpolar repulsions. FTIR results show that the characteristic 993 cm^{-1} stretching band of pyridine ring is completely shifted to 1008–1010 cm^{-1} , indicating essentially full complexation. Carboxylic acids behave differently, most likely due to the competing strong hydrogen-bonding interactions between these acids. FTIR shows that for P4VP complexed with dodecanoic acid, the 993 cm^{-1} band splits into two peaks, indicating that full complexation is not achieved. SAXS and WAXS data also support this conclusion. All three P4VP–alkyl carboxylic acid complexes show a distinct SAXS peak in the melt. Because birefringence is not observed, it is attributed to characteristic concentration fluctuations in an otherwise homogeneous state. This indicates that although the hydrogen bonding is strong enough, the polar–nonpolar repulsion is insufficient (note that P4VP-PDP is also already homogeneous above 60 $^{\circ}\text{C}$). Alternatively, the complexation is far from complete, due to the competing intermolecular hydrogen bonding between the carboxylic acid molecules.

Aliphatic alcohols with moderate chain length, such as dodecanol, yield some hydrogen bonding, manifested by the splitting of the 993 cm^{-1} FTIR band. However, no SAXS peak is observed in the melt. Longer aliphatic alcohols, such as hexadecanol and docosanol, give rise to liquid–liquid phase separation.

The phase behavior with respect to P4VP of the various surfactants studied can most conveniently be summarized according to the classification scheme given in section 3.1:

Alkylphenol surfactants: I, $T < T_{\text{ODT}}$; II, $T > T_{\text{ODT}}$

Alkyl carboxyl acid surfactants: II

Alkyl alcohol surfactants: III, $n \leq 12$; IV, $n \geq 16$

Alkylamine surfactants: IV

So far we have barely scratched the surface of these intriguing polymer–surfactant systems. Of the ones studied, the alkylphenol surfactants are most interesting with respect to the observation of order–disorder transitions and the resulting morphology. Although only lamellar structures have been observed so far by us (i.e., P4VP-PDP), various other structures should in principle also be possible. The unexpected behavior of the multifunctional LG surfactant suggests a different line of research involving mesomorphic structures and physical cross-linking. All these systems have one interesting element in common: a competition between the characteristic relaxation times. Here, theoretical developments are called for, and we hope to be able to address this in a future publication.

Acknowledgment. We acknowledge Milja Karjalainen of the University of Helsinki for the WAXS experiments, Maarit Taka of Neste Oy (Finland) for assistance with some of the FT-IR measurements, and Lars-Olof Pietilä and Lisbeth Ahjopalo for guidance in the computations by using Biosym software. The work has been supported by Finnish Academy, Technology Development Centre (Finland) and Neste Foundation.

References and Notes

- (1) Platé, N. A.; Shibaev, V. P. *Comb-Shaped Polymers and Liquid Crystals*; Plenum Press: New York, 1987.
- (2) For a review of polymer liquid crystallinity, see: Brostow, W. *Polymer* **1990**, *31*, 979.
- (3) Österholm, J.-E.; Laakso, J.; Hänninen, S.; Mononen, P. U.S. Patent 5,151,221, 1992.
- (4) Chen, S. A.; Ni, J. M. *Macromolecules* **1992**, *25*, 6081.
- (5) Hsu, W. P.; Levon, K.; Ho, K. S.; Myerson, A. S.; Kwei, T. K. *Macromolecules* **1993**, *26*, 1318.
- (6) Ballauf, M. *Makromol. Chem. Rapid Commun.* **1986**, *7*, 407.
- (7) Ballauf, M. *Liq. Cryst.* **1987**, *2*, 519.
- (8) Damman, S. B.; Mercx, F. P. M.; Kootwijk-Damman, C. M. *Polymer* **1993**, *34*, 1891.
- (9) Wegner, G. *Makromol. Chem., Macromol. Symp.* **1986**, *1*, 151.
- (10) Kärnä, T.; Laakso, J.; Savolainen, E.; Levon, K. European Patent Application EP 0545 729 A1, 1993.
- (11) Levon, K.; Ho, K.-H.; Zheng, W.-Y.; Laakso, J.; Kärnä, T.; Taka, T.; Österholm, J.-E. *Polymer* **1995**, *36*, 2733.
- (12) Cao, Y.; Smith, P.; Heeger, A. J. U.S. Patent 5,232,631, 1993.
- (13) Vikki, T.; Ikkala, O. *Synth. Met.* **1995**, *71*, 235.
- (14) Cao, Y.; Smith, P. *Polymer* **1993**, *34*, 3139.
- (15) Ikkala, O. T.; Pietilä, L.-O.; Ahjopalo, L.; Österholm, H.; Passiniemi, P. J. *J. Chem. Phys.* **1995**, *103*, 9855.
- (16) Vikki, T.; Pietilä, L.-O.; Österholm, H.; Takala, A.; Ahjopalo, L.; Toivo, A.; Levon, K.; Passiniemi, P.; Ikkala, O. *Macromolecules* **1996**, *29*, 2945.
- (17) Antonietti, M.; Conrad, J.; Thünemann, A. *Macromolecules* **1994**, *27*, 6007.
- (18) Antonietti, M.; Conrad, J. *Angew. Chem., Int. Ed. Engl.* **1994**, *33*, 1869.
- (19) Antonietti, M.; Burger, C.; Effing, J. *Adv. Mater.* **1995**, *7*, 750.
- (20) Ikkala, O. T.; Ruokolainen, J.; ten Brinke, G.; Torkkeli, M.; Serimaa, R. *Macromolecules* **1995**, *28*, 7088.
- (21) Fredrickson, G. H. *Macromolecules* **1993**, *26*, 2825.
- (22) Ruokolainen, J.; Ikkala, O. T.; ten Brinke, G.; Torkkeli, M.; Serimaa, R. *Macromolecules* **1995**, *28*, 7779.
- (23) Eisenberg, A.; King, M. *Ion-Containing Polymers*; Academic Press: New York, 1977.
- (24) Ruokolainen, J.; ten Brinke, G.; Ikkala, O. T.; Torkkeli, M.; Serimaa, R. *Macromolecules* **1996**, *29*, 3409.
- (25) Brandys, F. A.; Bazuin, C. G. *Chem. Mater.* **1992**, *4*, 970.
- (26) Tal'roze, R. V.; Kuptsov, S. A.; Sycheva, T. I.; Bezborodov, V. S.; Platé, N. A. *Macromolecules* **1995**, *28*, 8689.
- (27) Ruokolainen, J.; Torkkeli, M.; Serimaa, R.; Komanshek, B. E.; Ikkala, O.; ten Brinke, G. *Phys. Rev. E.*, in press.
- (28) Ten Brinke, G.; Ruokolainen, J.; Ikkala, O. T. *Europhys. Lett.* **1996**, *35*, 91.
- (29) Arichi, S. *Bull. Chem. Soc. Jpn.* **1966**, *39*, 439.
- (30) Berkowitz, J. B.; Yamin, M.; Fuoss, R. M. *J. Polym. Sci.* **1958**, *28*, 69.
- (31) Vahvaselkä, S. *Report Series in Physics*; HUP-257, University of Helsinki, Finland, 1992.
- (32) Insight User Guide, Biosym Technologies, San Diego, 1993.
- (33) De Gennes, P. G. *Scaling concepts in polymer physics*; Cornell University Press: Ithaca, NY, 1979.
- (34) Leibler, L. *Macromolecules* **1980**, *13*, 1602.
- (35) Bates, F. S.; Fredrickson, G. H. *Annu. Rev. Phys. Chem.* **1990**, *41*, 525.
- (36) Benoit, H.; Hadzioannou, G. *Macromolecules* **1988**, *21*, 1449.
- (37) Cesteros, L. C.; Meaurio, E.; Katime, I. *Macromolecules* **1993**, *26*, 2323.
- (38) Cesteros, L. C.; Isasi, J. R.; Katime, I. *Macromolecules* **1993**, *26*, 7256.
- (39) Cesteros, L. C.; José, L.; Katime, I. *Polymer* **1995**, *36*, 3183.
- (40) Takahashi, H.; Mamola, K.; Plyler, E. K. *J. Mol. Spectrosc.* **1966**, *21*, 217.
- (41) Lee, J. Y.; Painter, P. C.; Coleman, M. M. *Macromolecules* **1988**, *21*, 954.

MA951800A